

Received July 8, 2020, accepted July 19, 2020, date of publication July 23, 2020, date of current version July 31, 2020.

Digital Object Identifier 10.1109/ACCESS.2020.3011031

Two-Dimensional New Communication Technology for Networked Ammunition

FAN ZHOU¹, FANGFANG FAN¹, YUEQIU JIANG¹, AND YONGXIN FENG¹

¹School of Information Science and Engineering, Shenyang Ligong University, Shenyang 110159, China

²Harvard Medical School, Harvard University, Cambridge, MA 02215, USA

Corresponding author: Yongxin Feng (fengyongxin@263.net)

This work was supported in part by the General Project of Education Department of Liaoning Province under Grant LG201914, and in part the National Defense Basic Scientific Research Planed Project (2018).


ABSTRACT In order to improve the transmission data rate and the three-resistance characteristics of the network ammunition communication link, this paper proposes a new communication technology with two dimensions. In this technology, orthogonal frequency division multiplexing (OFDM) is used for one-dimensional data transmission, and the G-function-driven subcarrier frequency change rule in differential frequency hopping (DFH) is used for two-dimensional data transmission, which breaks through the conventional idea of using carrier amplitude frequency phase modulation information, and establishes a new two-dimensional communication model based on DFH-OFDM. The theoretical analysis and simulation results show that the proposed two-dimensional new communication technology, without changing the original communication system and signal characteristics, effectively reduces the probability of signal interception, improves the communication system capacity, and has good three-resistance performance.

INDEX TERMS Networked ammunition, two-dimension, DFH, OFDM, DFH-OFDM.

I. INTRODUCTION

Wireless sensor network (WSN) is a wireless network composed of a large number of static or mobile sensors in a self-organizing and multi-hop manner [1]. It cooperatively senses, collects, processes and transmits the information of the perceived objects in the geographical area, and finally sends the information to the owner of the network [2], [3]. With the rapid development of Internet of things technology, future computer systems and wireless sensor networks, networked munitions emerge as the times require and play a crucial role in the battlefield [4], [5]. Networked ammunition is an ammunition that can be propelled by its own power device, can receive combat grid information during flight, and can automatically detect, track, locate the target, strike and damage the assessed ammunition [6]. In order to exert the operational effectiveness of networked ammunition on the informationized battlefield, it is a basic guarantee to establish an efficient, secure and reliable data communication link. This link can enhance the ability to deal with time-sensitive targets and improve task flexibility and situational awareness [7]. Networked ammunition communication link is mainly responsible for

the ground remote control signal is sent to the network of the ammunition, and the networked ammunition flight parameter sensors for remote sensing information and on-board sensors mission information transmission to the ground station, the communication between the ground station and network ammunition to transmit data based on the content, can be divided into the remote sensor data link link, telemetry link and tasks [8]. In view of the similarity of the working mechanism between the network ammunition and the unmanned aerial vehicle (UAV) communication system [9], [10], the key technologies used in the UAV communication link can be directly transplanted to the network ammunition communication link [11], [12]. In literature 9 and 10, orthogonal frequency division multiplexing (OFDM) technology is proposed to be applied to UAV communication link to meet the requirements of high speed and high reliability. In literature 11 and 12, Quad-Phase Shift Keyed (QPSK) technology is proposed to meet the requirements of high-definition video transmission waveform design of UAV communication link. Although both technologies are applicable to networked ammunition communication link, OFDM and QPSK technology are difficult to synchronize and have poor anti-interference, respectively These problems are the main factors that restrict the reliability of communication link [13]–[15].

The associate editor coordinating the review of this manuscript and approving it for publication was Rongbo Zhu .

Considering that the networked ammunition needs to transmit a large number of instructions and data to each other and to the support platform when carrying out tasks [6]. The information transmission rate required for the transmission of task instructions, control data, shared video and image data between the networked ammunition is also increasing with the application requirements. So the networked ammunition needs to have a higher data transmission rate to ensure the network High efficient collaborative control, task allocation and information sharing among chemical munitions. Further, in order to better adapt to the future electromagnetic spectrum warfare, higher requirements are placed on the networked ammunition communication link, that is, the communication link not only has high reliability, concealment and security, but also needs to meet the demand of high dynamic and high rate. Therefore, based on the existing anti-jamming communication system, this paper proposes a new two-dimensional communication technology based on DFH-OFDM from the perspective of time-frequency code domain fusion. This technology can support higher data transmission rate and anti-interference ability than OFDM. The main innovations of this paper are as follows:

- 1) The technology utilizes each subcarrier in OFDM to modulate one-dimensional data, and simultaneously uses the frequency variation rule of the subcarrier to carry the two-dimensional data, thereby realizing the two-dimensional data transmission and effectively improving the transmission data rate.
- 2) Based on the communication system and signal characteristics of the original communication system, the technology uses the multi-dimensional statistical characteristics of the signal to transmit information. The time-frequency domain characteristics of the instantaneous signal are unchanged, and the adjacent subcarrier frequency variation law carries the two-dimensional data is not easy to find and has strong concealment.
- 3) The technology drives the variation rule of the subcarrier frequency according to the two-dimensional data to be transmitted, and the randomness of the subcarrier increases the anti-interference of the communication process and reduces the probability of interception of the signal.
- 4) The bit error rate of two-dimensional data has a great impact on the total bit error rate of DFH-OFDM signals. Therefore, in the following work, the linear block code theory will be used to explore the correlation function between one-dimensional data and two-dimensional data, so as to reduce the influence of two-dimensional data error rate on the total bit error rate of signal, and further improve the anti-noise performance of DFH-OFDM signal.

The remainder of this paper is organized as follows: Section II elaborates on Proposed Scheme and two-dimensional new communication technology working

mechanism; Section III introduces presents the results of our experiments, and Section IV offers a conclusion.

II. PROPOSED SCHEME

A. TWO-DIMENSIONAL NEW COMMUNICATION TECHNOLOGY WORKING MECHANISM

The realization of the new two-dimensional communication technology is based on the OFDM technology. Starting from the control subcarrier channel selection and time-domain characteristics, the frequency control of the subcarriers is completed by the fanout coefficient of the G function in the DFH [16]–[18]. As far as the sender is concerned, the two-dimensional information data to be transmitted is set to be $D_1(n)$ and $D_2(n)$, respectively, and the information to be transmitted is transformed according to the modulation order and the G function operation rule [19], $D_1(n) \rightarrow S_1(m)$, $D_2(n) \rightarrow S_2(m)$. Where $S_1(m)$ and $S_2(m)$ are the symbols corresponding to $D_1(n)$ and $D_2(n)$, respectively, and the symbol length depends on the modulation order and the fanout coefficient of the G-function respectively. Two-dimensional information data modulation mapping association is shown in Fig. 1.

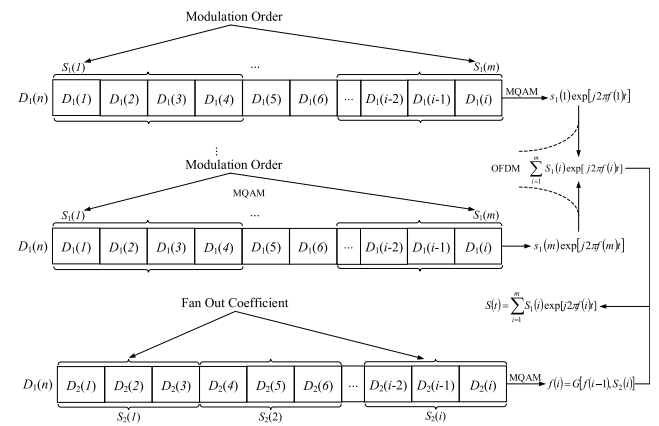


FIGURE 1. Schematic diagram of modulation mapping of bi-dimensional information data based on DFH-OFDM.

When the G function fanout coefficient is equal to 2, according to the G function rule, the relationship between the subcarrier frequency $f(i)$ and the two-dimensional data $D_2(n)$ can be established, as shown in the formula (1). Similarly, when the G function fanout coefficient is greater than 2, according to the G function rule, the relationship between the subcarrier frequency $f(i)$ and the symbol $S_2(m)$ corresponding to the two-dimensional data $D_2(n)$ can be established, as shown in the formula (2).

$$f(i) = G[f(i-1), D_2(i)] \quad (1)$$

$$f(i) = G[f(i-1), S_2(i)] \quad (2)$$

Further, the symbol $S_1(m)$ corresponding to the one-dimensional data $D_1(n)$ is modulated onto each subcarrier $f(i)$ generated by the corresponding symbol $S_2(m)$ of the

two-dimensional data $D_2(n)$, and a bidirectional modulation signal based on DFH-OFDM can be generated, and the time domain signal expression is shown in formula (3).

$$S(t) = \sum_{i=1}^m S_1(i) \exp[j2\pi f(i)t] \quad (3)$$

As far as receiver is concerned, the DFH-OFDM bi-dimensional modulation signal at time t is first subjected to FFT processing, and its expression is shown in formula (4).

$$S(\omega) = \sum_{i=1}^m S(t) \exp[-j2\pi f(i)t] \quad (4)$$

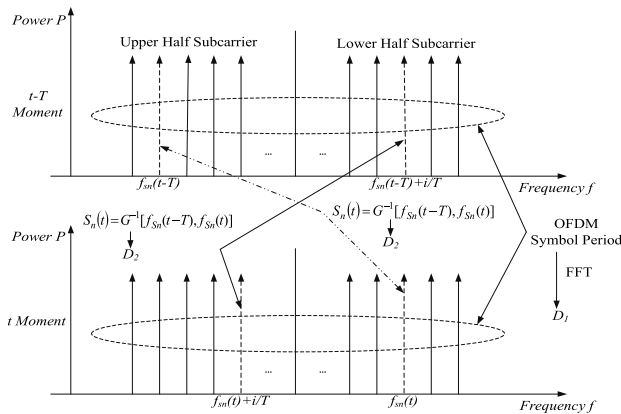


FIGURE 2. FFT based subcarrier frequency detection schematic diagram.

Secondly, it is assumed that the symbol period of the DFH-OFDM bi-directional modulation signal is T , and the frequency point detection is performed on the result of the FFT processing, the OFDM subcarrier set used for transmitting the data symbols at the time t is obtained, as shown in the formula (5). A schematic diagram of FFT-based subcarrier frequency detection is shown in Fig. 2.

$$\dots f(m) f(m-2) f(1) \dots \quad (5)$$

Further, set the time corresponding to the previous DFH-OFDM symbol of the current DFH-OFDM symbol corresponding to the time t is $t - T$, the $S_2(m)$ can be recovered according to the detected subcarrier frequency and the G^{-1} function between the preceding and succeeding symbols, and then passed $S_2(m)$ gets $D_2(n)$. Finally, $S_1(m)$ is obtained by demodulating the one-dimensional data symbols carried by the subcarriers, and then the transmitted one-dimensional data $D_1(n)$ is obtained by using $S_1(m)$. The rules for the association of G^{-1} functions with data are.

$$S_2(m) = G^{-1}[f_{t-T}(m-1), f_t(m)] \quad (6)$$

In the implementation of the new dual-dimensional communication technology based on DFH-OFDM, OFDM modulation is adopted for one-dimensional data, and MQAM (Multiple-Quadrature Amplitude Modulation) modulation is used for each symbol in the subcarrier [20]–[22].

Further, considering the orthogonality of the N subcarriers of the OFDM signal, the anti-noise performance of the OFDM signal can be equivalent to the sum of the anti-noise performance of the N MQAM signals [23], [24]. Without loss of generality, it is assumed that the number of subcarriers corresponding to the OFDM signal is N , each subchannel adopts MQAM modulation, and the bit error rate corresponding to each subchannel is P_M [25], [26], and the bit error rate calculation process of the MQAM modulated signal is as follows:

Suppose the MQAM signal corresponding to each subchannel can be expressed as:

$$e_{MQAM}(t) = \sum_{n=-\infty}^{+\infty} A_n g(t - nT_s) \cos(\omega_c t + \phi_n) \quad (7)$$

In the formula, A_n is the amplitude of the baseband signal, and $g(t - nT_s)$ is the baseband signal waveform of the n th symbol having the pulse width T_s , and ϕ_n is the carrier phase corresponding to the n th code element. Further, the orthogonal expression corresponding to the formula (7) is:

$$\begin{aligned} e_{MQAM}(t) &= \left[\sum_{n=-\infty}^{+\infty} A_n g(t - nT_s) \cos \phi_n \right] \cos \omega_c t \\ &\quad - \left[\sum_{n=-\infty}^{+\infty} A_n g(t - nT_s) \sin \phi_n \right] \sin \omega_c t \\ &= \left[\sum_{n=-\infty}^{+\infty} X_n g(t - nT_s) \right] \cos \omega_c t \\ &\quad - \left[\sum_{n=-\infty}^{+\infty} Y_n g(t - nT_s) \right] \sin \omega_c t \end{aligned} \quad (8)$$

where $X_n = A_n \cos \phi_n$, $Y_n = A_n \sin \phi_n$ are the n th code element amplitudes, and $\sum_{n=-\infty}^{+\infty} X_n g(t - nT_s)$ and

$\sum_{n=-\infty}^{+\infty} Y_n g(t - nT_s)$ are baseband signals.

In general, the MQAM signal constellation is in a rectangular form. For a rectangular signal constellation diagram under $M = 2^k$ (k is an even number), the MQAM signal constellation is equivalent to two PAM (Pulse Amplitude Modulation) signals on the orthogonal carrier signal [27]–[29]. Each of these two signals has $\sqrt{M} = 2^{k/2}$ signal points [30]–[32]. Since the signal on the phase quadrature component can be separated by the coherent decision method, the bit error rate of the MQAM can be determined by the bit error rate of the PAM [33]–[35]. The probability that the MQAM signal is correctly determined can be expressed.

$$p_C = \left(1 - P_{\sqrt{M}}\right)^2 \quad (9)$$

where $P_{\sqrt{M}}$ is the bit error rate of the \sqrt{M} -ary PAM system, which has an average power of half of each orthogonal signal of the equivalent MQAM system [36]–[38]. The bit error rate

of the \sqrt{M} -ary PAM system can be obtained by the bit error rate of the M -ary PAM system as.

$$P_{\sqrt{M}} = 2 \left[1 - \frac{1}{\sqrt{M}} Q \left(\frac{3}{M-1} \frac{E_s}{n_0} \right) \right] \quad (10)$$

where n_0 represents the average signal-to-noise ratio of each symbol, E_s represents the symbol energy, and n_0 represents the unilateral power spectral density of Gaussian white noise, so the bit error rate of MQAM is:

$$P_M = 1 - \left(1 - P_{\sqrt{M}} \right)^2 \\ = 1 - \left(1 - 2 \left[1 - \frac{1}{\sqrt{M}} Q \left(\frac{3}{M-1} \frac{E_s}{n_0} \right) \right] \right)^2 \quad (11)$$

Further, if the bit error rate of the OFDM signal is set as P_e^1 , the bit error rate of OFDM signal with MQAM modulation can be regarded as the sum of the bit error rate corresponding to N subchannels [39]–[41], that is:

$$P_e^1 = NP_M \\ = N \left\{ 1 - \left(1 - 2 \left[1 - \frac{1}{\sqrt{M}} Q \left(\frac{3}{M-1} \frac{E_s}{n_0} \right) \right] \right)^2 \right\} \quad (12)$$

The two-dimensional data is transmitted by the DFH differential frequency hopping system, and the corresponding bit error rate P_e^2 is:

$$P_e^2 = \sum_{n=1}^{N'-1} (-1)^{n+1} C_{N'-1}^n \frac{1}{n+1} e^{-\gamma m/n+1} \quad (13)$$

From the DFH-OFDM transmission mechanism, when the two-dimensional data $D_2(n)$ demodulation has an error, the one-dimensional data $D_1(n)$ is partially wrong demodulated at the time of demodulation; when the two-dimensional data $D_2(n)$ is demodulated without error, the one-dimensional data $D_1(n)$ may be wrong demodulated too [42]–[44]. Let the number of subcarriers participating in the hopping be N_1 , and the fanout coefficient of the G function in DFH be BPH. Therefore, the bit error rate P_e corresponding to the DFH-OFDM based two-dimensional communication signal can be expressed as:

$$P_e = \left(1 - P_e^2 \right) P_e^1 + P_e^2 \left[\frac{(N - N_1)}{(2^{BPH} - 1)N} \right] \quad (14)$$

In summary, the bit error rate corresponding to the DFH-OFDM signal is:

$$P_e = \left(1 - \sum_{n=1}^{N-1} (-1)^{n+1} C_{N-1}^n \frac{1}{n+1} e^{-\gamma m/n+1} \right) \\ N \left\{ 1 - \left(1 - 2 \left[1 - \frac{1}{\sqrt{M}} Q \left(\frac{3}{M-1} \frac{E_s}{n_0} \right) \right] \right)^2 \right\} \\ + \left[\sum_{n=1}^{N-1} (-1)^{n+1} C_{N-1}^n \frac{1}{n+1} e^{-\gamma m/n+1} \right] \left[\frac{(N - N_1)}{(2^{BPH} - 1)N} \right] \quad (15)$$

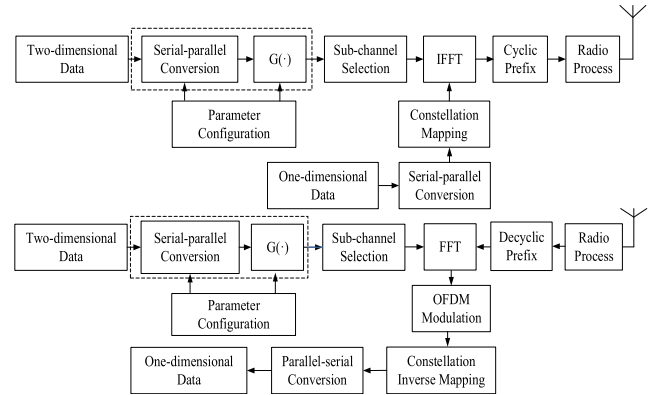


FIGURE 3. Two-dimensional new communication model based on DFH-OFDM.

B. TWO-DIMENSIONAL NEW COMMUNICATION TECHNOLOGY IMPLEMENTATION

Based on the transmission mechanism of the new two-dimensional communication technology, a new two-dimensional communication model based on DFH-OFDM is established, as shown in Fig. 3. The sender first configures the fanout coefficient of the G function according to the two-dimensional data $D_2(n)$, thereby completing the mapping relationship between the two-dimensional data $D_2(n)$ and the subcarriers, and further performing the serial-to-parallel conversion, the constellation mapping, and the IFFT transformation on the one-dimensional data $D_1(n)$, Successively, then generating a DFH-OFDM signal. The receiver performs recovery of the one-dimensional data $D_1(n)$ by FFT, subchannel detection, constellation inverse mapping, and parallel-to-serial conversion, and further recovers the two-dimensional data $D_2(n)$ by subcarrier detection and G^{-1} function.

According to the new dual-dimensional communication model based on DFH-OFDM, the workflow of transmitting and receiving signals in the technology can be described. Thereinto the signal generation workflow is shown in Fig. 4. The workflow is described as follows:

Step 1. First set the one-dimensional data rate R_1 , the two-dimensional data rate R_2 . Determining the fanout coefficient and the number of subchannels of the G function, requiring the number of subchannels to be greater than the fanout coefficient;

Step 2. Serial-to-parallel conversion of one-dimensional data and two-dimensional data by means of the number of subchannels and the fanout coefficient of the G function;

Step 3. Performing constellation mapping on the one-dimensional data serial-to-parallel conversion result;

Step 4. Selecting a subchannel according to the result of the serial-to-parallel conversion of two-dimensional data, and establishing a subcarrier carrying the two-dimensional data;

Step 5. Perform IFFT processing by using the constellation mapping and the selection result of the subchannel to generate a DFH-OFDM bidirectional modulation signal.

Step 6. Add a cyclic prefix to the DFH-OFDM dual-dimensional modulated signal.

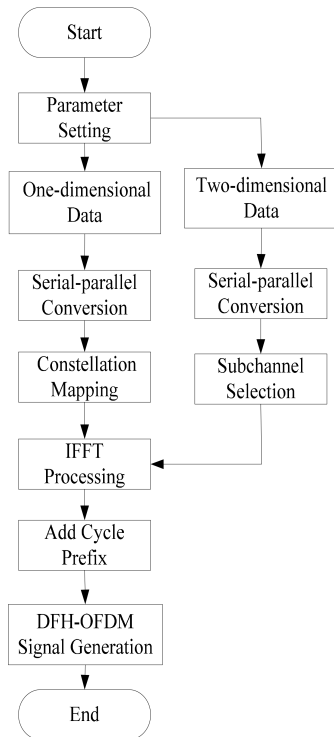


FIGURE 4. Signal generation workflow.

Step 7. Generate a DFH-OFDM dual-dimensional RF signal after radio frequency processing.

The signal receiving workflow is shown in Fig. 5. The workflow is described as follows:

Step 1. Perform radio frequency preprocessing on the received DFH-OFDM dual-dimensional modulated signal;

Step 2. Perform parameter configuration;

Step 3. De-cyclically prefix the received DFH-OFDM dual-dimensional modulated signal;

Step 4. Performing FFT processing on the two-dimensional signal of DFH-OFDM after the cyclic prefix is removed;

Step 5. Perform subchannel detection according to the result of the FFT processing;

Step 6. Demodulate the OFDM symbol by using the subchannel detection result;

Step 7. performing constellation inverse mapping on the demodulated OFDM symbol;

Step 8. performing parallel-to-serial conversion on the result of constellation inverse mapping;

Step 9. Deinterleaving the result of the parallel-to-serial conversion to recover the one-dimensional data;

Step 10. Solving the G^{-1} function by means of the subchannel detection result;

Step 11. Perform parallel-to-serial conversion on the output of the G^{-1} function to recover the two-dimensional data.

III. PERFORMANCE EVALUATION

A. SIGNAL GENERATION SIMULATION AND VERIFICATION

In the simulation, the communication link oriented to networked ammunition is used as the simulation object, and

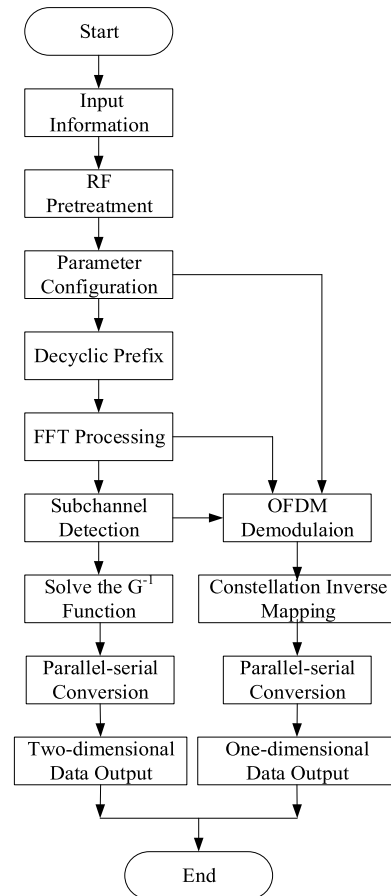
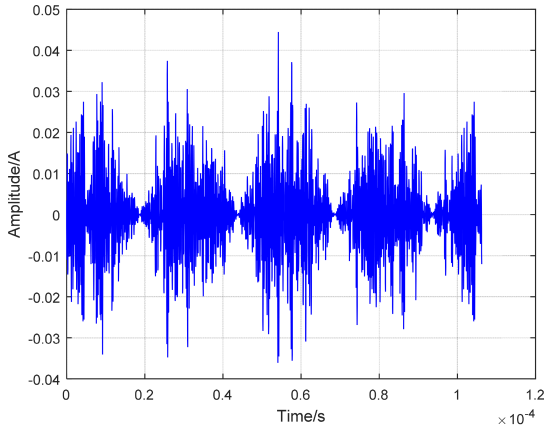


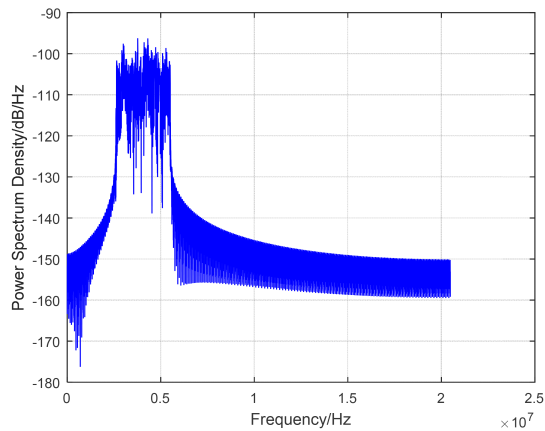
FIGURE 5. Signal receiving workflow.

the modulation mode 16QAM, IFFT point number is 2048, the sampling frequency is 40.96MHz, the subcarrier hopping frequency is 5000Hz, the fanout coefficient is 2. The number of subchannels is 144, the number of subcarriers is 288, the number of null subcarriers is 144, the one-dimensional data rate is 2.88 Mbps, the two-dimensional data rate is 720 Kbps, and the subcarrier frequency sequence number is 260-547. Matlab is used as a simulation tool to effectively verify the new two-dimensional communication technology.

Through simulation, the simulation results of the new two-dimensional communication signal based on DFH-OFDM are shown in Fig. 6. In the figure, (a)~(b) are the time domain and frequency domain simulation results respectively when the fanout coefficient is equal to 2. It can be seen that the number of frequency points included in each hop of the two-dimensional new communication signal based on DFH-OFDM is equal to the number of subcarriers, and a peak occurs at each subcarrier frequency point; when the fan-out coefficient is 2, the number of carrying one-dimensional data subcarriers is equal to the number of null subcarriers, and the number of participating hopping subcarriers is equal to the number of null subcarriers. At this time, the DFH-OFDM signal bandwidth is equal to 2.88 MHz, which is consistent with the DFH-OFDM based composite dimension signal generation requirement.



(a)The time domain results



(b)Power spectrum result

FIGURE 6. Simulation results of two-dimensional new communication signals based on DFH-OFDM.

B. SIGNAL RECEIVING SIMULATION AND VERIFICATION

Considering the high dynamics of the communication link of networked ammunition, the Rice channel is used as the transmission medium in the simulation process, the Rice factor is set to 50, and the time domain result of the channel output DFH-OFDM signal is shown in Fig. 7; The FFT processing result of the receiver’s two-dimensional new communication signal based on DFH-OFDM for two consecutive hops is shown in Fig. 8. The simulation results show that the number of FFT peak detection sequences equals the number of subcarriers is 144, which proves the correctness of the simulation results of the new two-dimensional communication signal based on DFH-OFDM after receiving and processing unit.

Further, the single-hop subcarrier frequency point detection result is shown in Table 1. It can be seen that through the subcarrier detection of FFT processing results of the current hopping signal, the frequency point set of the current hopping signal is obtained, and combined with the previous hop signal frequency point set and the G^{-1} function, the two-dimensional data can be parsed; Aiming at the demodulation of the dimensional signal can use the same demodulation method as the OFDM signal.

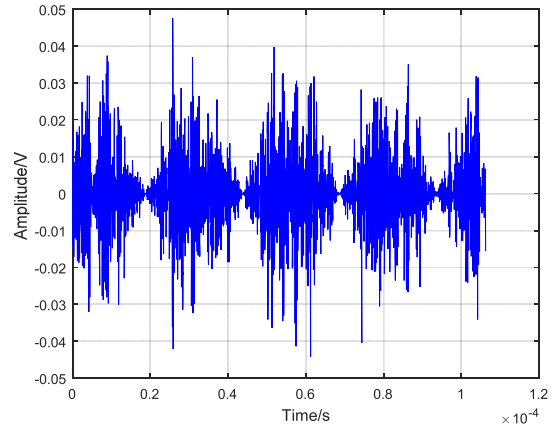


FIGURE 7. Time domain results of the Rice channel output.

TABLE 1. Single-hop subcarrier frequency point detection and two-dimensional data analysis results.

Subcarrier Number	Fan out	Test Content	Result Data
288	2	Current Hop Signal Frequency Point Set	404 405 262 407 408 265 266 411 412 413 270 415 416 273 418 275 276 421 422 423 424 281 426 427 428 429 430 287 432 289 434 291 292 293 294 439 440 297 442 299 300 301 446 447 304 305 306 451 452 453 310 455 456 313 314 315 460 317 462 319 464 321 466 467 468 469 470 327 328 329 474 331 476 333 478 335 336 337 482 339 340 485 486 487 488 345 490 491 348 493 350 351 496 497 498 355 500 357 358 359 360 505 362 507 364 509 366 511 512 513 370 371 372 517 374 519 520 521 378 379 380 525 382 527 528 529 386 387 388 533 390 535 392 393 394 395 540 541 542 399 544 545 402 547
		Previous Hop Signal Frequency Point Set	{260 261360 361.....461 462.....546 547}
		Two-dimensional Data	1 1 0 1 1 0 0 1 1 1 0 1 1 0 1 0 0 1 1 1 (Take 20bit for example)

After simulation, the demodulation results of the new two-dimensional communication signals based on DFH-OFDM are shown in Fig. 9. In the figure, (a) to (b) correspond to the one-dimensional data and two-dimensional data demodulation simulation results respectively when the fanout coefficient is equal to 2. Based on the current set of frequency hopping points and the previous set of hopping points, the G^{-1} function is used to demodulate to get the two-dimensional data, and the one-dimensional data is obtained according to the FFT processing. When the fanout coefficient is 2, the two-dimensional data rate is 720 Kbps, and the system transmission rate R_b is increased by 25%.

Anti-noise performance analysis of two-dimensional new communication technology. The fanout coefficient is set as 2,

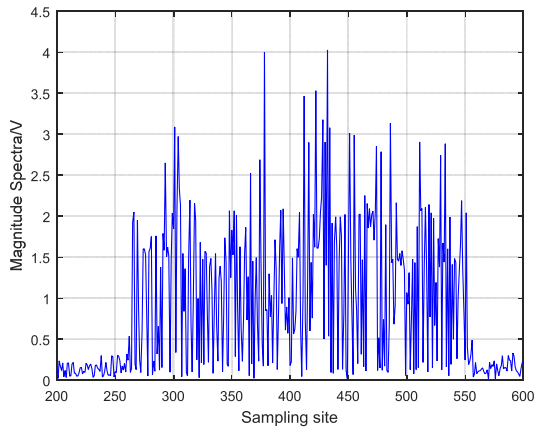


FIGURE 8. FFT processing results.

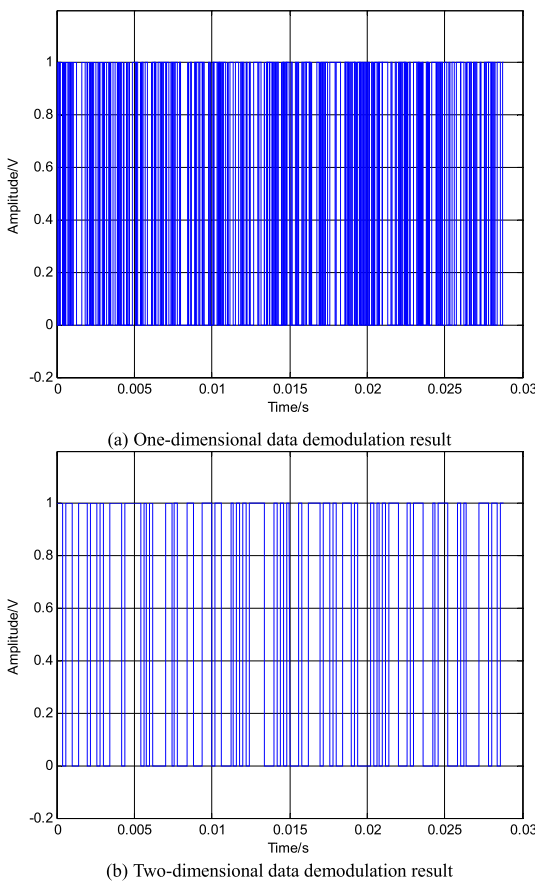


FIGURE 9. Demodulation results of a new two-dimensional communication signal based on DFH-OFDM.

and the number of subcarriers participating in the hopping is equal to 144. The anti-noise performance analysis of DFH-OFDM and OFDM signals is completed under the condition of AWGN channel and the same simulation parameters, as shown in Fig. 10. Simulation results show that under the same conditions of bit error rate, The one-dimensional data E_b/N_0 corresponding to the two-dimensional new communication method based on DFH-OFDM is consistent with E_b/N_0 corresponding to the OFDM transmission method; The total bit error rate corresponding to the two-dimensional

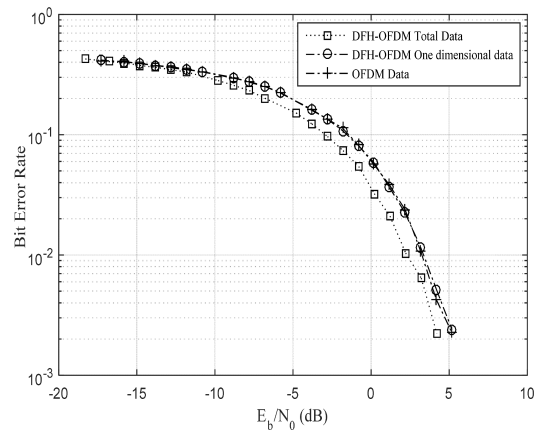


FIGURE 10. Anti-noise performance analysis of DFH-OFDM and DFH.

new communication method based on DFH-OFDM is about 0.3 dB higher than that corresponding to OFDM transmission method E_b/N_0 ; E_b/N_0 will further decrease as the number of participating hopping subcarriers decreases.

IV. CONCLUSION

In order to improve the data transmission rate and reliability of the networked ammunition communication link, it is better adapted to the needs of future electromagnetic spectrum warfare. Based on the traditional anti-jamming communication system, this thesis proposes a new two-dimensional communication technology based on DFH-OFDM, and analyzes the transmission mechanism, implementation method and anti-noise performance of the technology. The simulation results show that the technology can effectively improve the capacity of communication system and the anti-jamming performance is good, which can meet the working requirements of network ammunition communication link.

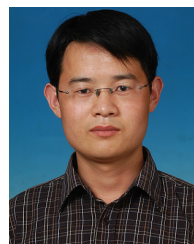
ACKNOWLEDGMENT

(Fan Zhou and Fangfang Fan contributed equally to this work.)

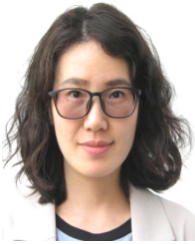
REFERENCES

- [1] W. Zhang, G. Han, X. Wang, M. Guizani, K. Fan, and L. Shu, "A node location algorithm based on node movement prediction in underwater acoustic sensor networks," *IEEE Trans. Veh. Technol.*, vol. 69, no. 3, pp. 3166–3178, Mar. 2020.
- [2] W. Zhang, L. Li, G. Han, and L. Zhang, "E2HRC: An energy-efficient heterogeneous ring clustering routing protocol for wireless sensor networks," *IEEE Access*, vol. 5, pp. 1702–1713, 2017.
- [3] X. Liu, R. Zhu, A. Anjum, J. Wang, H. Zhang, and M. Ma, "Intelligent data fusion algorithm based on hybrid delay-aware adaptive clustering in wireless sensor networks," *Future Gener. Comput. Syst.*, vol. 104, pp. 1–14, Mar. 2020.
- [4] Z. Huang, X. Xu, J. Ni, H. Zhu, and C. Wang, "Multimodal representation learning for recommendation in Internet of Things," *IEEE Internet Things J.*, vol. 6, no. 6, pp. 10675–10685, 2019.
- [5] R. Zhu, L. Liu, M. Ma, and H. Li, "Cognitive-inspired computing: Advances and novel applications," *Future Gener. Comput. Syst.*, vol. 109, pp. 706–709, Aug. 2020.
- [6] L. I. Ming, "Algorithm of networked ammunition attack decisionMaking based on AHP-TOPSIS," *Trans. Beijing Inst. Technol.*, vol. 37, no. 12, pp. 1315–1320, 2017.

- [7] H. U. Fei, "Research on precise direction-finding method for link 16 signal based on step deambiguity of dual channel phase difference," *Electron. Inf. Warfare Technol.*, vol. 34, no. 2, pp. 7–10, 2019.
- [8] D. Wang, "Accurate evaluation of explosive ammunition attacking target in actual combat," *Comput. Simul.*, vol. 35, no. 5, pp. 31–34, 2018.
- [9] L. Shao-Feng, W. Ning, G. Chao-Ping, and S. Yong-Hong, "Study on application of adoptive CP-OFDM in tactical UAV downlink transmission," in *Proc. Int. Conf. Smart Grid Electr. Autom. (ICSGEA)*, Jun. 2018, pp. 368–372, doi: [10.1109/ICSGEA.2018.00098](https://doi.org/10.1109/ICSGEA.2018.00098).
- [10] Q. Gao, "Design of UAV high resolution image transmission system," *Proc. SPIE Opt. Photon. Eng.*, vol. 10250, Feb. 2017, Art. no. 102502Y, doi: [10.1117/12.2266806](https://doi.org/10.1117/12.2266806).
- [11] M. Mustaqim, B. A. Khawaja, A. A. Razaqi, S. S. H. Zaidi, S. A. Jawed, and S. H. Qazi, "Wideband and high gain antenna arrays for UAV-to-UAV and UAV-to-ground communication in flying ad-hoc networks (FANETs)," *Microw. Opt. Technol. Lett.*, vol. 60, no. 5, pp. 1164–1170, May 2018.
- [12] J. Q. Xiong, L. C. Gan, and Y. C. Zhu, "Cooperative cognitive systems with orthogonal frequency division multiplexing and frequency hopping," *J. Electron. Inf. Technol.*, vol. 32, no. 12, pp. 3041–3045, 2016.
- [13] H. Ye, G. Y. Li, and B.-H. Juang, "Power of deep learning for channel estimation and signal detection in OFDM systems," *IEEE Wireless Commun. Lett.*, vol. 7, no. 1, pp. 114–117, Feb. 2018.
- [14] S. T. Wang, E. W. Hao, and G. C. Du, "Simulation analysis of anti-jamming performance of CHESS radio," *Ordnance Autom.*, vol. 34, no. 1, pp. 1–3, 2016.
- [15] S. Kamal, A. Cesar Azurda-Meza, and K. Lee, "Suppressing the effect of ICI power using dual sinc pulses in OFDM-based systems," *AEUE Int. J. Electron. Commun.*, vol. 70, no. 7, pp. 1312–1328, 2016.
- [16] L. Dong, Q. Guo, and W. Wu, "Speech corpora subset selection based on time-continuous utterances features," *J. Combinat. Optim.*, vol. 37, no. 4, pp. 1237–1248, May 2019.
- [17] F. S. Sahib, "Design and Analysis of an OFDM-Based Short Reference Quadrature Chaos Shift Keying Communication System," *Wireless Pers. Commun.*, vol. 1, no. 12, pp. 1–18, 2017, doi: [10.1016/j.ssci.2020.104838](https://doi.org/10.1016/j.ssci.2020.104838).
- [18] M. Zhang, "A probabilistic model of human error assessment for autonomous cargo ships focusing on human-autonomy collaboration," *Saf. Sci.*, vol. 130, Oct. 2020, Art. no. 104838, doi: [10.1016/2020.104838](https://doi.org/10.1016/2020.104838).
- [19] D. Jiang, G. Li, Y. Sun, J. Kong, and B. Tao, "Gesture recognition based on skeletonization algorithm and CNN with ASL database," *Multimedia Tools Appl.*, vol. 78, no. 21, pp. 29953–29970, Nov. 2019.
- [20] Y.-F. Shao, L. Chen, A.-R. Wang, Y.-J. Zhao, Y. Long, and X.-P. Ji, "Analysis of different sub-carrier allocation of M-ary QAM-OFDM downlink in RoF system," *Optoelectron. Lett.*, vol. 14, no. 1, pp. 40–43, Jan. 2018.
- [21] R. Tian, K. Senda, and H. Otsuka, "BER performance of OFDM-based 4096-QAM using soft decision Viterbi decoding in multipath fading," in *Proc. World Symp. Commun. Eng.*, 2018, pp. 1–4, doi: [10.1109/WSCE.2018.8690532](https://doi.org/10.1109/WSCE.2018.8690532).
- [22] S. Xu, X. Cao, G. Xu, and C. Tang, "Two classes of optimal frequency-hopping sequences with new parameters," *Appl. Algebra Eng., Commun. Comput.*, vol. 30, no. 1, pp. 1–16, Jan. 2019.
- [23] B. H. Dong, "The research of G-function decoding method for DFH system based on state trellis," in *Proc. Int. Conf. Commun. Mobile Comput.*, Apr. 2010, pp. 311–315, doi: [10.1109/CMC.2010.43](https://doi.org/10.1109/CMC.2010.43).
- [24] E. Bedeer, "Rate-interference tradeoff in OFDM-based cognitive radio networks," *IEEE Trans. Veh. Technol.*, vol. 64, no. 9, pp. 4292–4298, Sep. 2015, doi: [10.1109/GLOCOM.2014.7037279](https://doi.org/10.1109/GLOCOM.2014.7037279).
- [25] P. Sudharshan Babu, R. Budhiraja, and A. K. Chaturvedi, "Joint power allocation for OFDM-based non-concurrent two-way AF relaying," *IEEE Commun. Lett.*, vol. 22, no. 10, pp. 2100–2103, Oct. 2018, doi: [10.1109/LCOMM.2018.2858829](https://doi.org/10.1109/LCOMM.2018.2858829).
- [26] X.-R. Lv, Y. Li, and Y.-C. He, "Efficient impulsive noise mitigation for OFDM systems using the alternating direction method of multipliers," *Math. Problems Eng.*, vol. 2018, pp. 1–11, Jun. 2018, doi: [10.1155/2018/4968682](https://doi.org/10.1155/2018/4968682).
- [27] K. U. Chowdary and B. P. Rao, "Hybrid mixture model based on a hybrid optimization for spectrum sensing to improve the performance of MIMO-OFDM systems," *Int. J. Pattern Recognit. Artif. Intell.*, vol. 34, no. 07, Jun. 2020, Art. no. 2058008, doi: [10.1142/S0218001420580082](https://doi.org/10.1142/S0218001420580082).
- [28] K. Anoh, A. Ikpehai, K. Rabie, B. Adebisi, and W. Popoola, "PAPR reduction of wavelet-OFDM systems using pilot symbols," in *Proc. IEEE Int. Symp. Power Line Commun. Appl. (ISPLC)*, Apr. 2018, pp. 1–6, doi: [10.1109/ISPLC.2018.8360242](https://doi.org/10.1109/ISPLC.2018.8360242).
- [29] J. Shi, "Probabilistically shaped 1024-QAM OFDM transmission in an IM-DD system," *Opt. Fiber Commun. Conf.*, Mar. 2011, p. 44, doi: [10.1364/OFC.2018.W2A.44](https://doi.org/10.1364/OFC.2018.W2A.44).
- [30] L. Zhe, L. Xiao, and Q. Bo, "A method of LFM interference suppression for DFH communication based on FrFT," *Fire Control Command Control*, vol. 42, no. 2, pp. 25–33, 2017.
- [31] K. Chen-Hu and R. P. Leal, "Reducing the interference by adapting the power of OFDM for mMTC," in *Proc. VTC*, Jun. 2018, pp. 1–5, doi: [10.1109/VTCSpring.2018.8417533](https://doi.org/10.1109/VTCSpring.2018.8417533).
- [32] Z. Kaiming, "60GHz optical millimeter wave OFDM-RoF system based on DFT spread spectrum," *Opt. Commun. Technol.*, vol. 43, no. 3, pp. 36–39, 2019.
- [33] X. U. Tian-Tian, L. U. Han-Yu, and M. Kuan-Peng, "Research and Simulation of multi-carrier OFDM System," *Comput. Knowl. Technol.*, vol. 15, no. 14, pp. 259–261, 2019.
- [34] P. Panagoulas, I. Moscholios, G. Mariusz and M. Logothetis, "An analytical framework in ofdm wireless networks servicing random or quasi-random traffic," *Appl. Sci.*, vol. 24, no. 9, pp. 5365–5376, 2019.
- [35] A. Adnan, Y. Liu, C.-W. Chow, and C.-H. Yeh, "Demonstration of non-hermitian symmetry (NHS) IFFT/FFT size efficient OFDM non-orthogonal multiple access (NOMA) for visible light communication," *IEEE Photon. J.*, vol. 12, no. 3, Jun. 2020, Art. no. 7201405, doi: [10.1109/JPHOT.2020.2984564](https://doi.org/10.1109/JPHOT.2020.2984564).
- [36] Q. Yaojun, W. Lei, Z. Yuanzheng, and J. Yuefeng, "The simulation of optical beating interference avoidance scheme and system performance in orthogonal frequency division multiple address passive optical network system based on optical loop," *ACTA Photonica Sinica*, vol. 43, no. 7, 2014, Art. no. 706008, doi: [10.3788/gzxb20144307.0706008](https://doi.org/10.3788/gzxb20144307.0706008).
- [37] S. K. Pulariykodi et al., "Performance evaluation of OFDM based watermarking robust to multipath spatial shifts," *Int. J. Comput. Digit. Systemss*, vol. 7, no. 1, pp. 51–58, Jan. 2018, doi: [10.12785/ijcds/070106](https://doi.org/10.12785/ijcds/070106).
- [38] M. Zhang, D. Zhang, H. Yao, and K. Zhang, "A probabilistic model of human error assessment for autonomous cargo ships focusing on human-autonomy collaboration," *Saf. Sci.*, vol. 130, Oct. 2020, Art. no. 104838.
- [39] Y. Huang and B. Su, "Circularly pulse-shaped precoding for OFDM: A new waveform and its optimization design for 5G new radio," *IEEE Access*, vol. 6, pp. 44129–44146, 2018, doi: [10.1109/ACCESS.2018.2864336](https://doi.org/10.1109/ACCESS.2018.2864336).
- [40] A. Agarwal and P. Kumar, "Analysis of variable bit rate SOFDM based integrated satellite-terrestrial broadcast system in presence of CFO and phase noise," *IEEE Syst. J.*, vol. 13, no. 4, pp. 3827–3835, Dec. 2019, doi: [10.1109/JSYST.2018.2883659](https://doi.org/10.1109/JSYST.2018.2883659).
- [41] S. Yu-Feng, "Research on transmission characteristics of QAM-OFDM visible signals in Rayleigh fading channel," *J. Optoelectron. Laser*, vol. 30, no. 6, pp. 593–598, 2019.
- [42] X. Wang, X. Shen, and S. Ma, "A time-reversal based CP-free OFDM system for underwater acoustic communication," in *Proc. OCEANS*, Jun. 2019, pp. 1–6, doi: [10.1109/OCEANS.2019.8867179](https://doi.org/10.1109/OCEANS.2019.8867179).
- [43] S. H. H. Rafsanjani and S. Ghazi-Maghrebi, "Improving estimation of a sparse channel for OFDM systems by utilizing side information," in *Proc. Int. Symp. Netw., Comput. Commun. (ISNCC)*, Jun. 2019, pp. 1–6, doi: [10.1109/ISNCC.2019.8909139](https://doi.org/10.1109/ISNCC.2019.8909139).
- [44] A. Agarwal and P. Kumar, "Analysis of variable bit rate WH/CI-spread OFDM based integrated satellite-terrestrial broadcast system," *IET Commun.*, vol. 13, no. 6, pp. 786–795, Apr. 2019, doi: [10.1049/iet-com.2018.5337](https://doi.org/10.1049/iet-com.2018.5337).



FAN ZHOU received the M.E. degree from Shenyang Ligong University, Shenyang, China, in 2013, where he is currently pursuing the Ph.D. degree. He is currently an Associate Professor with the School of Information Science and Engineering, Shenyang Ligong University. He has published more than 20 papers in key academic journals and international conferences, and ten of them have been indexed by EI/SCI. He has also published one monographs and authorized four patents and five software copyrights. His research interests include wireless communication, signal processing, and data link technology.



FANGFANG FAN received the Ph.D. degree from the Huazhong University of Science and Technology, in 2013. She is currently a Research Fellow with Harvard University. Her current research interests include emotion regulation and mental health, and neural electrophysiology signal processing.



YUEQIU JIANG received the Doctor of Computer Applied Technology degree from Northeastern University, in 2004. She has worked with Shenyang Ligong University. She is currently a Professor. Her research interests include network transmission technology, signal processing, and network management technology.



YONGXIN FENG received the M.S. degree in computer science from Northeastern University, in 2000, and the Ph.D. degree in computer science and technology from the School of Information Science and Engineering, Northeastern University, in 2003. She is currently a Professor with Shenyang Ligong University. She has published more than 100 papers in key academic journals and international conferences, and 75 of them have been indexed by EI/SCI. She has also published seven monographs and one teaching material and authorized 16 patents and ten software copyrights. She has been selected into the National Millions of Talents Project, and has been rewarded as the Young and Middle-Aged Expert, the State Council Expert, the Outstanding Talent of the New Century in the Ministry of Education, and the Outstanding Expert of Liaoning Province. Her representative researching awards include the Second Prize for National Science and Technology Progress Awards and 11 Awards for Provincial and Ministerial Science and Technological Progress.

...